# Realization of stable ferromagnetic order in a topological insulator: Codoping-enhanced magnetism in 4f transition metal doped Bi_{2}Se_{3}

Bei Deng, Yiou Zhang, S. B. Zhang, Yayu Wang, Ke He, and Junyi Zhu

Phys. Rev. B **94**, 054113 — Published 26 August 2016

DOI: 10.1103/PhysRevB.94.054113

# Realization of Stable Ferromagnetic Order in Topological Insulator: Codoping Enhanced Magnetism in 4*f* Transition Metal Doped $Bi_2Se_3$

Bei Deng[1], Yiou Zhang[1], S. B. Zhang[2], Yayu Wang[3], Ke He[3] and Junyi Zhu[1,*]

[1]*Department of physics, the Chinese University of Hong Kong, Hong Kong SAR*

[2]*Department of Physics, Applied Physics, and Astronomy, Rensselaer Polytechnic Institute, Troy, New York 12180, USA*

[3]*Department of Physics, Tsinghua University, Beijing 100084, People's Republic of China*

The quantum anomalous Hall effect (QAHE), originates form a combination of the spin-orbital coupling and the breaking of time-reversal symmetry due to intrinsic ferromagnetic ordering, was recently observed in Cr- and V-doped magnetic topological insulators (TI). However, it was only observed at extremely low temperatures due to the low ferromagnetic Curie temperature and tiny magnetically-induced gap. To fully understand the mechanism of the ferromagnetic ordering whereby improving the ferromagnetism, we investigated 4*f* transition-metal-doped $Bi_2Se_3$, using density-functional-theory approaches. We predict that Eu and Sm can introduce stable long-range ferromagnetic states in $Bi_2Se_3$, with large magnetic moments and low impurity disorders .Additionally, codoping is proposed to tune the Fermi level into the gap, which simultaneously improve the magnetic moment and the incorporation of magnetic ions. Our findings thus offer a critical step in facilitating the realization of QAHE in TI systems.

PACS numbers: 71.20.Nr, 61.72.U-, 75.50.Pp

## I. INTRODUCTION

The Quantum Hall effect (QHE), characterized by the quantized Hall conductance, with the formation of Laudau levels under an external magnetic field, was observed in two-dimensional electron systems more than 30 years ago[1,2]. As first proposed by Haldane[3], by circulating currents loop on a honeycomb lattice, the QHE can exist even without the external magnetic field and the formation of Laudau levels, namely the Quantum anomalous Hall effect (QAHE). However, the Haldane model is difficult to realize experimentally. Later, numerous models were proposed to realize QAHE in realistic materials, including magnetically doped quantum wells[4-7], transition metal oxide heterostructures [8–13], grapheme /silicene [14-19], magnetic topological insulator (TI) thin films [20-26], etc. [27-29]. However, the QAHE was only reported to be successful in Cr- and V-doped $(Bi,Sb)_2Te_3$ magnetic TI thin films[30-36].

The key idea for the realization of QAHE is to introduce the time-reversal symmetry (TRS) breaking perturbations, e.g. a ferromagnetic order in topological insulators, usually by doping the TI with magnetic impurities [30-36]. The introduced exchange splitting can destroy the band inversion in one of the spin channels, whilst keeping the nontrivial band topology in the other spin channel due to the spin-orbital coupling, which opens up a finite gap at the Dirac point and lead to the QAHE [37]. The reason for chose the TI system, especially the $Bi_2Se_3$ family which has been proved successful in QAHE, is that besides its strong SOC and a single-surface Dirac cone, the ferromagnetic orders can be derived directly from the large Van Vleck spin susceptibility in the host without the mediation of itinerant carriers[24], which eventually makes the QAHE being possible. However, the QAHE observed from recent experimental observations typically occurs at extremely low temperatures because of the low Curie temperature ($T_C$) and small magnetically-induced band gap[30-36], hindering its realistic applications. Therefore, of crucial importance is to find alternative magnetic impurities to increase the $T_C$ as well as the nontrivial band gap for QAHE.

3*d* transition metals (TMs), such as Cr and V, have proved successful in creating insulating ferromagnetic states in $Bi_2Se_3$ family for QAHE purpose. Besides these 3*d* TMs, the 4*f* TMs may be better candidates for introducing ferromagnetic orders in $Bi_2Se_3$. First, as the 4*f* TMs have ionic radii larger than the 3*d* TMs, they will match the $Bi_2Se_3$ lattice better than the 3*d* TMs do, naturally giving rise to smaller distortion and therefore less disorder. Also, the 4*f* bands typically have a more localized character and should be less interactive than the 3*d* bands. This could be beneficial in avoiding the impurity aggregation that have been observed in Cr-doped $(Bi,Sb)_2Te_3$[38], which are responsible for the magnetic disorders, Indeed, our first-principles calculations further confirmed such expectation, given that the 4*f* impurity (e.g. Nd) is favorable to distribute uniformly in the $Bi_2Se_3$ lattice to form a long-range order, while the 3*d* TM (e.g. Cr) has a tendency of aggregating. Another advantage of the 4*f* TMs should be attributed to their large atomic mass, which enables stronger SOC with respect to 3*d* TMs, and this will probably lead to larger magnetically-induced band gap, together with stronger FM order due to the van Vleck mechanism [24]. Furthermore, *f* bands normally have two more electronic orbitals than *d* bands, so that they are able to introduce larger magnetic moment which is crucial to enhance the quantized Hall conductance plateau in QAHE [39]. Until now, however, a systematic investigation is still lacking.

In this letter, to address the above questions, we investigated the 4*f* TMs-doped $Bi_2Se_3$, by *ab-initio* calculations based on density functional theory (DFT). We confirmed that the 4*f* TM impurities are energetically more favorable to stay on the Bi substitution sites than the 3*d* TM impurities are, revealing a suppression of impurity disorders. Among these 4*f* TMs, several of

them can introduce large magnetic moments and be strongly coupled in the FM states. Typically, Eu and Sm show large magnetic moments of 6.33 and 5.06 $\mu$B, respectively, both with strong FM character. The calculated FM coupling strength is about 3-4 times larger than that of Cr impurity, as reported in previous works [40]. Besides, Tb and Dy are also energetically favorable to introduce large magnetic moments, whose coupling favors moderately-stable FM states. Moreover, to realize insulating FM states for QAHE, we proposed that by codoping donor impurities with the magnetic ions, such as Eu, the Fermi level can be tuned into the gap, and the magnetic moments and the incorporation of the magnetic ions can be simultaneously enhanced. These findings can have important implications on the realization of the QAHE.

## II. COMPUTATIONAL METHOD AND DETAILS

In this study, we use the VASP code [41], with spin polarized generalized gradient approximation (GGA) and Perdrew-Burke-Enzerhof (PBE)[42] functional for exchange-correlation. Projected augmented wave (PAW) pseudopotentials [43] for Bi, Se and 4*f* TMs were used with a planewave basis-set cutoff energy of 300 eV, while 4*f* states and 5*d* states were included in the valence. Spin-orbital coupling (SOC) was included in the total energy and electronic structure. Besides the PBE functional, we also considered the screened Hartree-Fock hybrid density functional (HSE06) [44] and GW approximation [45] to test the general applicability of the PBE results. It shows that the formation energies of the 4*f* impurities given by PBE, HSE, and GW differ by less than 5%, which reveals the reliability of the PBE functional for this study. The $Bi_2Se_3$ has a rhombohedral structure composed of three weakly coupled quintuple layers (QLs). In order to maintain a reasonable interaction among the QLs, we included the van der Waals interaction in the calculation [46], and obtained the lattice constants $a$ = 4.19 Å and $c$ = 28.54 Å, which can be compared to experimental values $a$ = 4.14 Å and $c$ = 28.64 Å [47]. The geometry of isolated impurities was modeled by using a 60-atom supercell, consisting of 2×2×1 conventional $Bi_2Se_3$ cells in the hexagonal lattice. A Γ-centered 7×7×2 Monkhorst-Pack mesh was used for *k*-point sampling in the Brillouin zone. In obtaining the geometry, all the atoms are allowed to relax until the calculated Hellmann-Feynman forces are less than 5 meV/Å.

We calculated the formation energy of TM impurity on the Bi site ($TM_{Bi}$), various interstitial sites ($TM_i$), and the Se site ($TM_{Se}$) of $Bi_2Se_3$, which allows us to investigate the spin-dependent electronic structure of the impurities. The defect formation energy is defined as [48]:

$$\Delta H_f(TM) = E_{tot}(Bi_2Se_3:TM) - E_{tot}(host) - \sum_i n_i\mu_i \qquad (1)$$

where $E_{tot}$ ($Bi_2Se_3$:TM) is the total energy of a supercell containing one charge neutral impurity; $E_{tot}$ (host) is the total energy of the defect-free supercell; $n_i$ is the number of atoms of a certain element added to ($n_i < 0$) or removed from ($n_i > 0$) the supercell; and $\mu_i$ is the chemical potential of that element. The *chemical potentials* should fulfill the following conditions: i) $2\mu_{Bi} + 3\mu_{Se} = \Delta H_f(Bi_2Se_3)$ to keep the host material thermodynamically stable; ii) $x\mu_{TM} + y\mu_{Se} \leq \Delta H_f$ ($TM_xSe_y$) to avoid formations of secondary phases of $TM_xSe_y$, and iii) $\mu_i < 0$ to avoid precipitations of elementary substances for both host and TM elements.

## III. THE FORMATION OF 4F IMPURITIES IN $Bi_2Se_3$

We first consider the TMs at the interstitial sites and substitutional Se sites, as these impurities, $TM_i$ and $TM_{Se}$, often cause impurity disorders with large changes in the electronic structure, whereby leading to a deterioration of the magnetic ordering, and hence should be avoided. Our calculations reveal that the 4*f* impurities are unlikely to occupy these detrimental sites. Consider for example, the $TM_i$s. There are two types of them in the $Bi_2Se_3$ lattice, namely, the octahedral and tetrahedral sites, each with 6 different configurations. We have examined all of them and found that the most stable one is on the octahedral site between two QLs. Yet, it's significantly more difficult to form $TM_i$ than to form $TM_{Bi}$, as the formation energy of $TM_i$ is at least 1.08 eV higher than that of $TM_{Bi}$ at the most favorable Bi-rich conditions. This difference is noticeably larger than the reported 0.29 eV for the 3*d* TM impurities [40], showing that the 4*f* TMs are energetically more favorable on the Bi sites, which reveals an improvement against the impurity disorders as in the 3*d* TM doped case, due to the relatively large sizes of the 4*f* TMs that better match Bi than the 3*d* TMs do.

Next, we examine eight selected $TM_{Bi}$ impurities, which are Nd, Sm, Eu, Gd, Tb, Dy, Ho, and Er. The calculated formation energies are shown in Fig. 1, as a function of the Se chemical potential. Except for $Eu_{Bi}$, $Sm_{Bi}$ and $Ho_{Bi}$, the calculated formation energies are always negative, regardless the growth conditions. This is in line with experimental observation that a number of the 4*f* elements can form continuous alloy with $Bi_2Se_3$ and/or $Bi_2Te_3$ [49-52]. It is noted that Eu and Gd have a significantly large formation energy difference (> 1.3eV), even though they are adjacent neighbors in the Periodic Table. As this difference cannot be understood solely by the atomic-size difference, we have studied the effect of atomic chemical potentials on the formation of these impurities (see Fig. 2). We found that to avoid the formation of secondary phases, in particular, TM selenides, the maximum chemical potential of Eu is -4.11 eV, which is 0.43 eV lower than

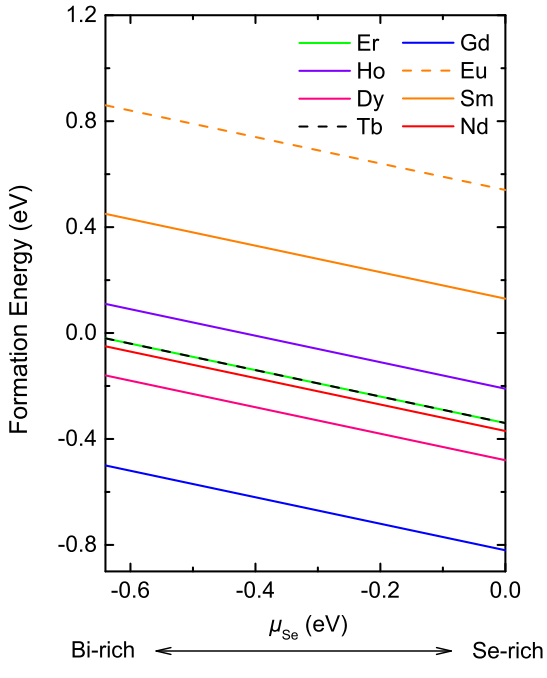


FIG. 1. Calculated formation energy of eight $TM_{Bi}$ impurities, as a function of the chemical potential of Se.

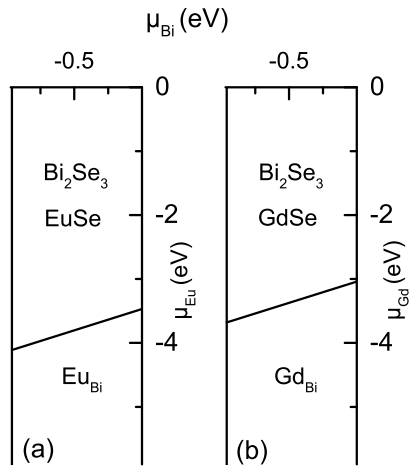


FIG. 2. Available equilibrium chemical potential regions calculated for (a) $Eu_{Bi}$ and (b) $Gd_{Bi}$ in $Bi_2Se_3$ system, in the two dimensional plane. The horizontal axis shows the chemical potential of Bi and vertical axis indicates the chemical potential of the impurities.

that of Gd (-3.68 eV), at equilibrium. The reason for a lower chemical potential of Eu lies in its exceptionally stable secondary phase EuSe, where Eu has a valence +2, leaving behind with a very stable half-occupied *f* band, according to the Hund's rule. The lower chemical potential for Eu here is consistent with the larger impurity formation energy. The remaining formation energy difference between Eu and Gd may be attributed to their different electronic structures – while $Gd_{Bi}$ has occupied *f* bands deeply buried inside the valence band, $Eu_{Bi}$ has its partially occupied bands near the Fermi level, and hence $Eu_{Bi}$ cannot be nearly as stable as $Gd_{Bi}$.

## IV MAGNETIC CHARACTERS OF THE 4F IMPURITIES

Due to the crystal field splitting [53,54] in $Bi_2Se_3$, the *f* bands of the $TM_{Bi}$ impurities may split by coupling to the *p* states of the host, which lowers the *f* band degeneracy. At the same time, if the system has a spin-degenerate ground state, the spin-up levels will have an exchange interaction with the spin-down levels, leading to an exchange splitting between the two, thereby lowering the total energy of the system. Assuming that the exchange splitting is larger than the crystal field splitting, the *f* orbitals are most likely to be occupied by electrons of parallel spin, leading to a high-spin configuration with large magnetic moment; otherwise, the electrons will have higher tendency to occupy the levels with anti-parallel spin, giving rise to a low-spin ground state. To investigate such magnetic behavior, we calculated the magnetic moments for all 4*f* TMs and listed the results in TABLE I. These results suggest that while the crystal filed splitting of those 4*f* impurities is generally weak in $Bi_2Se_3$, the corresponding exchange splitting is relatively large, which is preferred for the QAHE. We note that among all the candidates, $Gd_{Bi}$ and $Eu_{Bi}$ have the largest magnetic moments, being 7$\mu$B and 6.33$\mu$B, respectively, in the direction perpendicular to $Bi_2Se_3$ QLs. These values are greater than the maximum of 5$\mu$B ever possible for 3*d* TM impurities [40].

A stable long-range magnetic order depends not only on the local magnetic moment, but also on the coupling of the magnetic moments in the same direction. To estimate the magnetic coupling in a solid, one usually places two TM impurities in a supercell, with a set of different distances, and then calculate the magnetic coupling strength $\Delta E_{\text{FM-AFM}}/2$ (defined here as a half of the energy difference between the FM and AFM states). In this work, the magnetic configuration for ferromagnetic states is achieved by setting the two magnetic ions with the same and parallel spin, while the anti-ferromagnetic configuration is realized by setting the two magnetic ions having the same spin but with an anti-parallel direction. By using this approach, we found that the strongest magnetic coupling between TM impurities typically happens at the second-nearest-neighbor distance within the same QL (whose energy difference, when significant, is given in TABLE I) and decays at the third-nearest-neighbor distance (by about 15% per neighbor-distance which suggests an effective doping concentration of 7.5%), while the coupling of impurities between QLs can be noticeably smaller. The results show that the FM coupling is favorable in Sm- and Eu-doped $Bi_2Se_3$ and moderately favorable in Tb- and Dy-doped $Bi_2Se_3$, while the Er- and Gd-doped $Bi_2Se_3$ favors a weak AFM coupling. Note that massive Dirac fermion has been observed experimentally in Dy-doped $Bi_2Te_3$ up to room temperature [52], implying the TRS breaking due to the existence of an FM order. Nd in TABLE I represents a different case in which the nearest neighbor FM coupling (21 meV) is the strongest, but the second nearest neighbor coupling is only 1 meV.

To further our understanding, we then focus on the electronic band structure and projected density of states (PDOS), shown in Fig. 3(a)-(f), for Eu and Gd. Note that while the Gd-doping preserves the insulating nature of the $Bi_2Se_3$ host, the Eu-doping leads to a *p*-type character. Correspondingly, the band gap is calculated to be 79 and 30 meV, respectively, for Gd- and Eu-doped systems, larger than the reported 22 meV for the Cr-doped case[40]. This can be understood as a combined result of the *p*-*f* couplings near the valence band maximum (VBM) and the SOC. It is known that the 4*f* states are normally more localized than the 3*d* states, with a weaker coupling to the *p* states near the VBM. This is typified by the localized impurity states inside the band gap for Eu, as can be seen in Fig. 3(b) and (e). Moreover, for Gd, the impurity bands are much deeper, about -3.5 to -4.5 eV below the Fermi level, as revealed by Fig. 3(f), due to the extra *f* electron of Gd. While according to the Hund's rule, having 7 electrons half-occupying the *f* shell makes the Gd impurity very

TABLE I. Magnetic moments and magnetic coupling strengths ($\Delta E_{\text{FM-AFM}}/2$) of eight 4*f* TM impurities.

| Dopant | La | Ce | Pr | Nd | Sm | Eu | Gd | Tb | Dy | Ho | Er | Tm | Yb | Lu |
|---|---|---|---|---|---|---|---|---|---|---|---|---|---|---|
| Magnetic Moment ($\mu$B) | 0 | 0.71 | 1.95 | 3 | 5.06 | 6.33 | 7 | 6.01 | 4.99 | 3.98 | 2.92 | 1.90 | 0.76 | 0 |
| $\Delta E_{\text{FM-AFM}}/2$ (meV) | – | – | – | -1 | -44 | -31 | 2 | -14 | -14 | -10 | 3 | – | – | – |

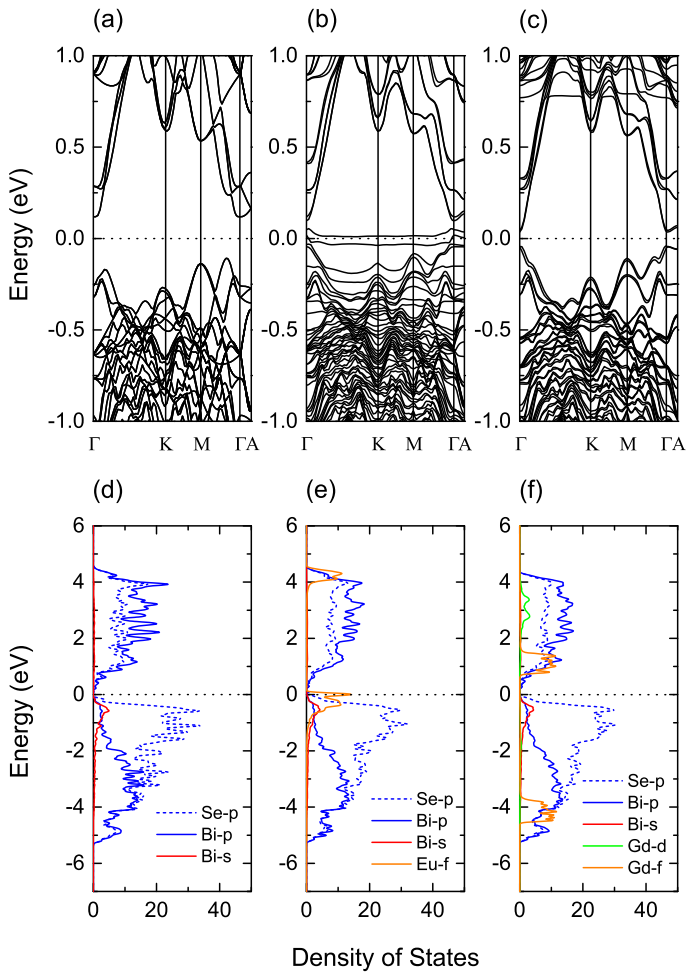


FIG. 3. Band structure for (a) pure, (b) Eu-doped, and (c) Gd-doped $Bi_2Se_3$ and PDOS for (d) pure, (e) Eu-doped, and (f) Gd-doped $Bi_2Se_3$. Fermi level is set to zero, as indicated by the dash lines. SOC has been included in the calculation.

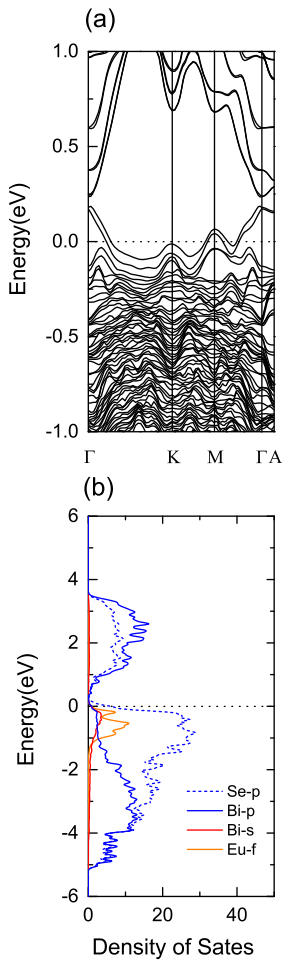


FIG. 4. Calculated (a) band structure and (b) projected density of sates for Eu doped $Bi_2Se_3$, using GGA+U approach. The Fermi level is set to zero, as indicated by the dash line. The SOC is also taken into account in the calculations.

stable, the lower *f* bands also make the *p*-*f* coupling less significant than the Eu-doped case, so the band gap of $Bi_2Se_3$:$Gd_{Bi}$ is also noticeably larger than $Bi_2Se_3$:$Eu_{Bi}$. Besides, owning to their larger atomic mass the 4*f* TMs, in contrast to 3*d* TMs, have reasonably stronger SOC with the host, which is also responsible for the obtained larger gaps. We note that whilst the electron correlation in GGA functional may underestimate the band gap, the implementation of on-site Columbic correction U could further enhance the gap, yet it may reduce the magnetic coupling [24,55]. To verify this, we have considered an on-site Columbic correction (GGA+U) to the 4*f* states of Eu. The on-site Columbic term was parametrized with U= 7 eV and J = 0.75 eV, respectively [56]. The electronic structure provided in Fig. 4 shows that the band gap is enhanced to 45 meV with the Columbic correction. However, simultaneously the magnetic coupling strength will undergo a reduction of about 17%,

The above band structures provide us with a qualitative picture for the obtained FM and AFM states in Eu- and Gd-doped $Bi_2Se_3$, which could also be extended to other systems. The strong FM coupling in Eu-doped system is suggested to originate from the exchange coupling between Eu impurities via the intervening Se atoms. The 4*f* states of Eu will exhibit splitting by coupling to the 4*p* states of Se under the approximate $O_h$ symmetry of the crystal field of $Bi_2Se_3$, resulting in higher-lying *p*-*f* hybridized $t_{1u}$ states and lower-lying $t_{2u}$ and $a_{2u}$ states, and then the $t_{1u}$ states could be further mixed with the higher relativistic 4*f*- 7/2 states, and the $t_{2u}$ and $a_{2u}$ be mixed with the lower relativistic 4*f*- 5/2 states, due to the spin-orbital coupling. Then the exchange splitting will give them a rigid shift, resulting in two impurity bands. In the FM states, the coupling between the impurity bands and the *p* states near the VBM lowers the lower-lying majority-spin states [see Fig. 5(a), the outmost panels], and raises the partially-occupied higher-lying majority- spin states near the Fermi level [see Fig. 5(a), the second outmost panels]. Then, coupling between the higher-lying impurity states, across the impurities [see Fig. 5(a), the middle panel] lowers the total energy of the system. In the AFM states, in contrast, coupling between the low-lying majority-spin states [i.e., those in Fig. 5(b), the outmost panels] and the high-lying unoccupied minority-spin states (in the conduction band) takes place [see Fig.

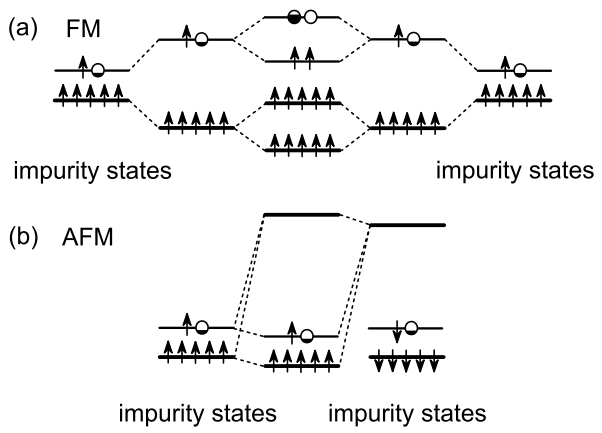


FIG. 5. Schematic illustration for the (a) ferromagnetic and (b) anti-ferromagnetic couplings in Eu-doped $Bi_2Se_3$.

5(b), the middle panel]. While such a coupling can also lower the total energy of the system, the exchange splitting between the majority and minority spins is quite large for the 4*f* impurities, which counteracts and leads to a smaller energy gain. Therefore, the FM state is the ground state in Eu-doped $Bi_2Se_3$. This, however, does not happen in Gd-doped system, because the majority-spin states of Gd are deep inside the valence band and merely weakly-coupled to the *p* states near the VBM, an FM coupling on such fully-occupied states cannot gain the system much energy. Instead, the AFM coupling will be more favorable. This rationale is supported by the calculated weak AFM state for Gd-doped $Bi_2Se_3$ in TABLE I, which also supports the recent experiment [49].

Moreover, we noticed here that Sm also favors a strong FM state, with a large magnetic moment of 5.06 $\mu$B and low formation energy of 0.12 eV. Also, the FM coupling strength for Sm ions is 44 meV, even stronger than for Eu. From a previous calculation by Chen *et al.*[57] and in conjunction with the calculated PDOS in Fig. 3(e) for $Eu_{Bi}$, we see that $Sm_{Bi}$ has an electronic structure similar to $Eu_{Bi}$, but with one less *f* electron. The coupling between the lower-lying fully-occupied impurity bands and the higher-lying partially-occupied impurity bands with one less electron generally should lead to a larger energy gain. These results provide strong evidence for the recent experiment [57], where stable FM state in 5% Sm-doped $Bi_2Se_3$ samples was observed at 52K.

## V. THE MAGNETIC CODOPING

For successful QAHE in a TI system, it requires that the magnetically-doped system remains to be insulating, and that the magnetic impurities have a sufficient concentration to achieve a long-range order. Therefore, for Eu- or Sm-doped $Bi_2Se_3$, to realize QAHE, it is essential to be able to raise the Fermi level into the band gap. One possible strategy is to incorporate with the TM the right amount of *n*-type dopants, such as group VII anions or group IV cations. As such a codoping can also change the band occupations, the magnetic moments and the magnetic coupling for the TM impurities. Its overall effect needs be addressed.

We then performed calculations on the Eu- and donor-codoped $Bi_2Se_3$ system. Considered for example, the Eu- and I-codoped system, the calculated electronic structures are shown in Fig. 6 (a) and (b). We noted that, accompanied with the lowering of the *f* bands of Eu, the Fermi level of the system shifts up into the band gap, and the gap is further enhanced to 55 meV (80 meV, with the inclusion of U), which is strongly preferred for the QAHE. This is attributed to the charge transfer from the donor's (I) *p* states to acceptor's (Eu) *f* states, which lowers the energy position of the *f* bands and in turn stabilizes the electronic structure of the system. Also, the lowering of the *f* bands reduces the *p*-*f* coupling at the VBM, which accounts for the obtained larger gap. Simultaneously, the Eu substitution will have relatively *larger* magnetic moments but reasonably *lower* ferromagnetic coupling strength, (see TABLE II). This suggests that the magnetic moments and their coupling can be sensitive to charge compensation induced by the donors. However, by our results the isolated donors cannot create magnetic moment in the absence of Eu, thus the enhanced magnetic moment cannot be interpreted in terms of the spin-spin interaction between the donors. Instead, we note that there is a charge transfer from the

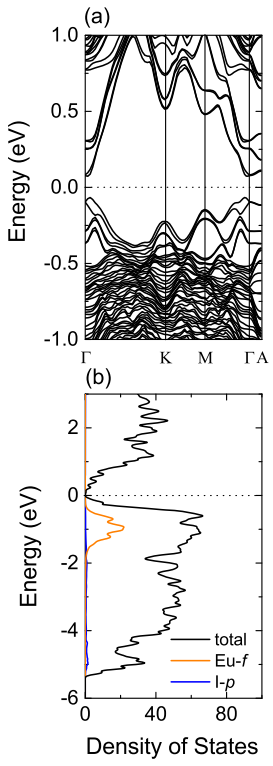


FIG. 6. The calculated electronic (a) band structure and (b) density of states for the Eu-I codoped $Bi_2Se_3$. The Fermi level is set to zero, as indicated by the dashed line. SOC is included in the calculation.

*p* states of the donors to the *s*, as well as the majority-spin *f* states of Eu, leading to different band occupations. A larger occupation of the $Eu_{Bi}$ majority-spin states results in the larger magnetic moment. On the down side, however, this charge transfer also leads to a larger occupation of the partially-occupied impurity states, whereby raising the total energy of the magnetically-coupled system and in turn lowering the coupling strength. This explains why the FM coupling strength of Eu is always lowered upon the codoping. Nonetheless, the donor-compensated Eu still has a reasonably strong FM coupling strength above 20 meV, suggesting

TABLE II. The calculated magnetic moment, magnetic coupling strength ($\Delta E_{FM\text{-}AFM}/2$) and formation energy (under Se-rich conditions) of $Eu_{Bi}$ codoped with group VII anions and group IV metallic cations, with the concentration at $x = y = 0.083$. As a matter of comparison, the corresponding results for the isolated $Eu_{Bi}$ are also given here.

| Host | Magnetic Moment ($\mu$B) | $\Delta E_{FM\text{-}AFM}/2$ (meV) | Formation Energy (eV) |
|---|---|---|---|
| $Bi_2Se_3$ | 6.33 | -31 | 0.54 |
| $Bi_2Se_{3-x}I_x$ | 6.88 | -26 | -0.24 |
| $Bi_2Se_{3-x}Br_x$ | 6.86 | -24 | -0.28 |
| $Bi_2Se_{3-x}Cl_x$ | 6.85 | -23 | -0.31 |
| $Bi_2Se_{3-x}F_x$ | 6.76 | -21 | -0.41 |
| $Bi_{2-y}Se_3Pb_y$ | 6.49 | -22 | 0.52 |
| $Bi_{2-y}Se_3Sn_y$ | 6.87 | -24 | 0.24 |
| $Bi_{2-y}Se_3Ge_y$ | 6.97 | -24 | 0.34 |

that the FM ground state of the Eu can be preserved, irrespective of the exact concentration of the donors. This insensitivity is due to the fact that the exchange coupling is mediated by spin-polarized holes *localized* at the impurity states, subject to bounded magnetic polarons (BMPs) [58-60], and the magnetism is further enhanced by the Van Vleck mechanism. To verify this, we subsequently performed calculations on a donor-compensated Sm impurity. The obtained FM coupling strength is also on the order of 20 meV, in line with the Eu results. In our view, however, $Sm_{Bi}$ may not be as promising as $Eu_{Bi}$ for realizing QAHE in $Bi_2Se_3$, because Sm has one less *f* electron than Eu and behaves as a double-donor, so two electron donors are needed to fully compensate one Sm. A recent experiment has demonstrated a ferromagnetism induced TRS breaking at the $Bi_2Se_3$-EuS interface [61], due to the strong exchange filed introduced by the magnetic proximity with the *insulating* EuS layer, so we believe that such FM states can also be established by Eu doping.

The remaining issue to be addressed is the incorporation of Eu, which is suspected to be more difficult than Cr, given that the calculated formation energy minimum is 0.54 eV, higher than that of Cr (about -0.25 eV) [40]. This, as we discussed earlier, can be understood in terms of the competitive secondary phase and the energy position of the *f* bands as well. Within the same way of codoping, unsurprisingly, the +2 valence of Eu can be retained, yet lower formation energy may be achieved. In particular, the formation energy of Eu can be lowered by 0.02-0.30 eV when codoped with cation donors, and can be lowered by 0.78-0.95 eV when codoped with anion donors. This is attributed to the charge transfer from the donor's *p* states to acceptor's (Eu) *f* states combined with a strain effect [62], which stabilize the electronic structure of the doped system and in turn improves the impurity solubility, and this can be further evidenced by analogical experiments [63-65]. Note that the formation energy of Eu generally can be lowered more when codoped with anion donors. A more significant reduction in the formation energy by the anion donors is because they have shorter distances to Eu, which is on the cation-Bi site. Thus, the anion donors can form a stronger binding with Eu due to Columbic attraction, which is the strongest for F. After all, Eu is still slightly smaller than Bi. Hence, a compressive stress on the host can be beneficial for its incorporation. In this regard, F has the smallest atomic radius and is expected to bring in the largest local compression effect on the host to enhance Eu incorporation.

## VI. CONCLUSIONS

In summary, our study confirms several 4*f* TMs as promising magnetic impurities for stable ferromagnetism in $Bi_2Se_3$. In startle contrast to widely-used 3*d* TMs, the 4*f* TMs are possible to introduce higher magnetic moments with larger exchange splitting, stronger FM orders, and lower impurity disorders. The observed magnetic order is proposed to originate form the *p-f* exchange coupling further combined with the Van Vleck mechanism. To establish insulating FM states for QAHE, codoping TMs with non-magnetic donor-like impurities was proposed as a means to tune the Fermi level into the gap and to enhance the solubility of the TM ions inside $Bi_2Se_3$.

## ACKNOWLEDGMENTS

This work is supported by direct grant from CUHK (4053084), ECS grant from HKRGC (ref No. 24300814) and startup funding from CUHK. SBZ was supported by the US Department of Energy (Office of Basic Energy Sciences) under Grant No. DE-SC00026 23.

## APPENDIX: THE GEOMETRIC DISTRIBUTION OF THE Cr SUBSTITUTION AND Nd SUBSTITUTION IN $Bi_2Se_3$

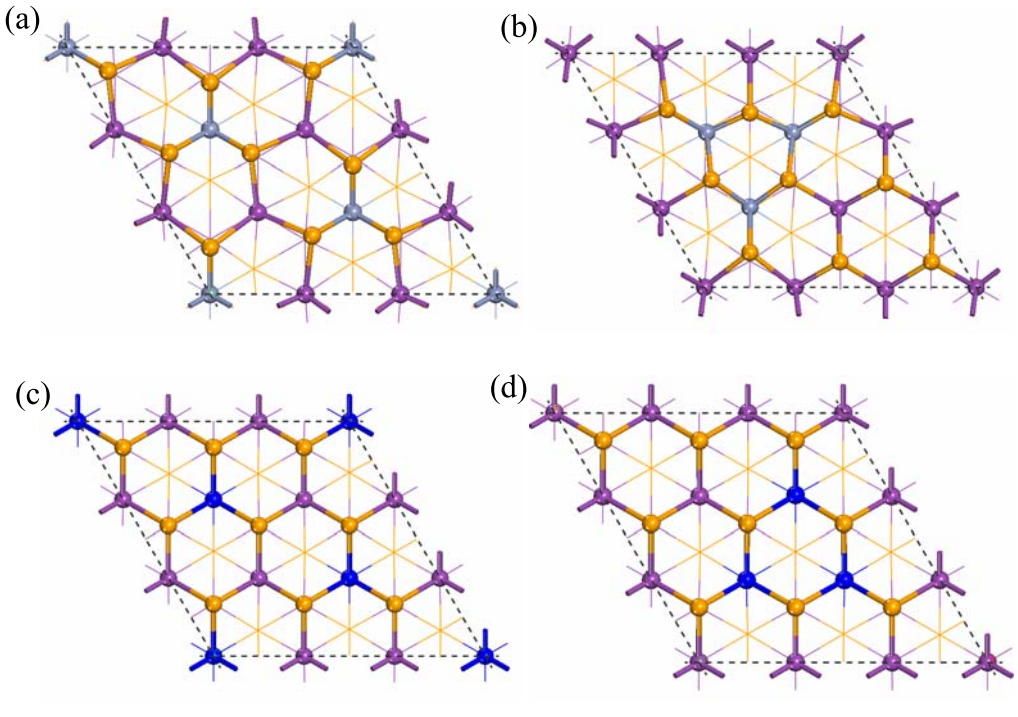


FIG. 7. The calculated geometric structure (top view) for Cr- and Nd-doped $Bi_2Se_3$ systems. (a) The geometry of the Cr-doped $Bi_2Se_3$, in which the Cr atoms are uniformly distributed, forming a long-range impurity order; (b) the geometry of the Cr aggregation (trimmer) in $Bi_2Se_3$, corresponding to a short-range impurity order. (c) The geometry of Nd-doped $Bi_2Se_3$ with a long-range impurity order, (d) the geometry of the Nd-doped $Bi_2Se_3$ with the short-range trimmer structure. The doping concentration in all above pictures is the same. The Se, Bi, Cr and Nd atoms are indicated by the purple, orange, gray and blue balls, respectively.

As observed by the recent experiment [38], the introduced 3*d* TM magnetic impurities, for instance Cr, tend to aggregate with each other to form a trimmer-like structure in $Bi_2Se_3$, giving rise to deterioration to the long-range ferromagnetic order. Our first-principles calculation further confirms such phenomenon, giving that the trimmer-like structure of Cr is energetically more stable than the long-range structure in which the Cr ions are uniformly distributed, with the total energy lower in an order of tens of meV. The reason for this can be understood as follows. First, as shown in Fig. 7 (a), the substitution of Cr ions on Bi site typically leads to a local distortion and a geometric symmetry breaking surrounding the ions, due to the large lattice mismatch, and such distortion can be suppressed by forming the aggregation structure [see Fig. 7(b)]. Second, the 3*d* bands of the Cr atoms are not sufficiently localized and are considered to be more active, so that these atoms have a tendency to bind together via the interaction between the 3*d* bands, which can lower the total energy of the system. However, such phoneme does not happen on the 4*f* TM impurities. Taking Nd for instance, in contrast to the above results, our calculation shows that the Nd atoms are energetically more favorable to be uniformly distributed in $Bi_2Se_3$, rather than forming the aggregation trimmers, with the energy gain being the order of twenties of meV. The reason for this, as can be seen from Fig. 7 (c,d), is that the 4*f* Nd substitutions do not introduce such a large distortion in $Bi_2Se_3$ as in 3*d* Cr-doped case, owning to that the Nd atoms reasonably match the $Bi_2Se_3$ lattice better. Moreover, the 4*f* bands of the Nd atoms are more localized and less interactive, and then the long-range magnetic coupling further enhances their stability.

---

*jyzhu@phy.cuhk.edu.hk

[1] K. Klitzing, G. Dorda, M. Pepper, Phys. Rev. Lett. 45, 494 (1980).
[2] D. C. Tsui, H. L. Stormer, A. C. Gossard, Phys. Rev. Lett. 48, 1559 (1982).
[3] F. D. M. Haldane, Phys. Rev. Lett. 61, 2015 (1988).
[4] C.-X. Liu, X.-L. Qi, X. Dai, Z. Fang, and S.-C. Zhang, Phys. Rev. Lett. 101, 146802 (2008).
[5] H.-C. Hsu, X. Liu, and C.-X. Liu, Phys. Rev. B 88, 085315 (2013).
[6] Q.Wang, X. Liu, H.-J. Zhang, N. Samarth, S.-C. Zhang, and C.-X. Liu, Phys. Rev. Lett. 113, 147201 (2014).
[7] H. Zhang, Y. Xu, J. Wang, and S.-C. Zhang, ar-Xiv:1402.5167.
[8] D. Xiao,W. Zhu, Y. Ran, N. Nagaosa, and S. Okamoto, Nat. Commun. 2, 596 (2011).
[9] A. Rüegg and G. A. Fiete, Phys. Rev. B 84, 201103(R) (2011).
[10] K.-Y. Yang, W. Zhu, D. Xiao, S. Okamoto, Z. Wang, and Y. Ran, Phys. Rev. B 84, 201104 (2011).
[11] F. Wang and Y. Ran, Phys. Rev. B 84, 241103 (2011).
[12] X. Hu, A. Rüegg, and G. A. Fiete, Phys. Rev. B 86, 235141 (2012).
[13] A. Rüegg, C. Mitra, A. A. Demkov, and G. A. Fiete, Phys. Rev. B 85, 245131 (2012).
[14] Z. Qiao, S. A. Yang, W. Feng, W.-K. Tse, J. Ding, Y. Yao, J. Wang, and Q. Niu, Phys. Rev. B 82, 161414 (2010).
[15] W.-K. Tse, Z. Qiao, Y. Yao, A. H. MacDonald, and Q. Niu, Phys. Rev. B 83, 155447 (2011).
[16] Z. Qiao, W. Ren, H. Chen, L. Bellaiche, Z. Zhang, A. H. MacDonald, and Q. Niu, Phys. Rev. Lett. 112, 116404 (2014).
[17] C.-C. Liu, W. Feng, and Y. Yao, Phys. Rev. Lett. 107, 076802 (2011).
[18] C.-C. Liu, H. Jiang, and Y. Yao, Phys. Rev. B 84, 195430 (2011).
[19] M. Ezawa, Phys. Rev. Lett. 109, 055502 (2012).
[20] Qi, X.-L.; Wu, Y.-S.; Zhang, S.-C. Phys. Rev. B 2006, 74, 045125.
[21] Qi, X.-L.; Hughes, T.; Zhang, S.-C. Phys. Rev. B 2008, 78, 195424.
[22] Liu, C.-X.; Qi, X.-L.; Dai, X.; Fang, Z.; Zhang, S.-C. Phys. Rev. Lett. 2008, 101, 146802.
[23] Li, R.; Wang, J.; Qi, X.-L.; Zhang, S.-C. Nat. Phys. 2010, 6, 284.
[24] Yu, R.; Zhang, W.; Zhang, H.-J.; Zhang, S.-C.; Dai, X.; Fang, Z. Science 2010, 329, 61.
[25] H. Jiang, Z. Qiao, H. Liu, and Q. Niu, Phys. Rev. B 85,045445 (2012).
[26] K. Nomura, N. Nagaosa, Phys. Rev. Lett. 106, 166802 (2011).
[27] K. F. Garrity and D. Vanderbilt, Phys. Rev. Lett. 110, 116802 (2013).
[28] C. Fang, M. J. Gilbert, and B. A. Bernevig, Phys. Rev. Lett. 112, 046801 (2014).
[29] F. Zhang, X. Li, J. Feng, C. Kane, and E. Mele, arXiv: 1309.7682.
[30] C.-Z. Chang, J. Zhang, X. Feng, J. Shen, Z. Zhang, M. Guo, K. Li, Y. Ou, P. Wei, L.-L. Wang, Z.-Q. Ji, Y. Feng, S. Ji, X. Chen, J. Jia, X. Dai, Z. Fang, S.-C. Zhang, K. He, Y. Wang, L. Lu, X.-C. Ma, and Q.-K. Xue, Science 340, 167 (2013).
[31] C.-Z. Chang, W. Zhao, D. Y. Kim, H. Zhang, B. A. Assaf, D. Heiman, S.-C. Zhang, C. Liu, M. H. W. Chan, and J. S. Moodera, Nat. Mater. 14, 473 (2015).
[32]J. G. Checkelsky, R. Yoshimi, A. Tsukazaki, K. S. Takahashi, Y. Kozuka, J. Falson, M. Kawasaki, and Y. Tokura, Nat. Phys. 10, 731 (2014).
[33]X. Kou, S.-T. Guo, Y. Fan, L. Pan, M. Lang, Y. Jiang, Q. Shao, T. Nie, K. Murata, J. Tang, Y. Wang, L. He, T.-K. Lee, W.-L. Lee, and K. L. Wang, Phys. Rev. Lett. 113, 137201 (2014).
[34]A. Kandala, A. Richardella, S. Kempinger, C.-X. Liu, and N. Samarth, Nat. Commun. 6, 7434 (2015).
[35] X. Kou, L. Pan, J. Wang, Y. Fan, E. S. Choi, W.-L. Lee, T. Nie, K. Murata, Q. Shao, S.-C. Zhang, and K. L. Wang, Nat. Commun. 6, 8474 (2015).
[36]Y. Feng, X. Feng, Y. Ou, J. Wang, C. Liu, L. Zhang, D. Zhao, G. Jiang, S.-C. Zhang, K. He, X. Ma, Q.-K. Xue, and Y. Wang, Phys. Rev. Lett. 115, 126801 (2015).
[37] X.-L. Qi and S.-C. Zhang, Rev. Mod. Phys. 83, 1057 (2011).
[38]C.-Z. Chang, P. Tang, Y.-L. Wang, X. Feng, K. Li, Z. Zhang, Y. Wang, L.-L. Wang, X. Chen, C. Liu, W. Duan, K. He, X.-C. Ma, and Q.-K. Xue, Phys. Rev. Lett. 112, 056801 (2014).
[39] J. Wang, B. Lian, H. Zhang, Y. Xu, and S. C. Zhang, Phys. Rev. Lett. 111, 136801 (2013).
[40] J. -M. Zhang, et al., Phys. Rev. Lett. 109, 266405 (2012).
[41] G. Kresse and J. Furthmuller, Phys. Rev. B 54, 11 169 (1996).
[42] J. P. Perdew, et al., Phys. Rev. Lett. 77, 3865 (1996).

[43] G. Kresse, & D. Joubert, Phys. Rev. B 59, 1758 (1999).
[44] A.V. Krukau, et al., J. Chem. Phys. 125, 224106 (2006).
[45] L. Hedin and S. Lundqvist, in Solid State Physics, edited by H. Ehrenreich, F. Seitz, and D. Turnbull (Academic, New York, 1969), Vol. 23.
[46] A. Tkatchenko, et al., Phys. Rev. Lett. 102, 073005 (2009).
[47] S. Nakajima, J. Phys. Chem. Solids 24, 479-485 (1963).
[48] C. G. Van de Walle et al., J. Appl. Phys. 95, 3851 (2004).
[49] S. W. Kim, et al., Appl. Phys. Lett. 106, 252401 (2015).
[50] S. Li, et al., Appl. Phys. Lett. 102, 242412 (2013).
[51] S. E. Harrison, et al., J Appl. Phys. 115, 023904 (2014).
[52] S. E. Harrison, et al., Sci. Rep. 5, 15767 (2015).
[53] W. A. Harrison, Electronic Structure and The Properties of Solids, (Dover Publications, Mineola, NY, USA, 1989).
[54] B. Huang et al., Phys. Rev. Lett.108, 206802 (2012).
[55] K. Sato, P. H. Dederichs, H. Katayama-Yoshida, J. Kudrnovsky, Physica B 340-342, 863 (2003).
[56] J. Kuneš and R. Laskowski, Phys. Rev. B 70, 174415 (2004).
[57] T. Chen, et al., Adv. Mater. 33, 4823 (2015)
[58] J. B. Torrance, et al., Phys. Rev. Lett. 29, 1168 (1972).
[59] A. Kaminski and S. Das Sarma, Phys. Rev. B 68, 235210 (2003).
[60] Y. Tian et al., Appl. Phys. Lett. 98, 162503 (2011).
[61] P. Wei, F. Katmis, B. Assaf, H. Steinberg, P. Jarillo-Herrero, D. Heiman, and J. S. Moodera, Phys. Rev. Lett. 110, 186807 (2013).
[62] J. Zhu, F. Liu, G. B. Stringfellow, S.-H. Wei, Phys. Rev. Lett.105, 195503 (2010).
[63] I. S. Cho, et al., Nat. Commun. 4, 1723 (2013).
[64] M. Chiodi, et al., J. Phys. Chem. C 116, 311 (2012).
[65] S. H. Park, et al., J. Appl. Phys. 108, 093518 (2010).